# EFFECTS OF ELECTRIC FIELDS ON HEAT-PIPE CHARACTERISTICS

M. K. Bologa, L. L. Vasil'ev,
I. A. Kozhukhar', and V. D. Shkilev

UDC 537.248.2:537.212

Here we consider some features of the effects of electric fields [1] on the thermal and hydrodynamic characteristics of heat pipes.

1. Electroosmotic Heat Pipes. The hydrodynamic head $\Delta P$ and speed v of the liquid in an electroosmotic pump with cylindrical capillaries are given by

$$\Delta P = \frac{4\varepsilon_0\varepsilon\xi U}{d^2}, \tag{1}$$

$$v = \frac{\varepsilon_0\varepsilon\xi U}{8\eta l}, \tag{2}$$

where these formulas have been derived from the equality of the Coulomb force at the double boundary layer at the capillary wall [2] and the viscous resistance for small values of the Reynolds number [3]. Equations (1) and (2) apply provided that the pore diameters do not differ too greatly from the thickness of the double layer.

In the case of a wick with pores of more complex shape, the formulas for $\Delta P$ and v should not differ greatly from those of (1) and (2); with $\varepsilon_0\varepsilon = 10^{-9}$ F/m, $\xi = 0.05$ V, $U = 10^3$ V, and $d = 10^{-5}$ m we get $\Delta P = 2\cdot10^3$ N/m$^2$, which constitutes a large fraction of $\Delta P$ for an ordinary capillary pump. In fact, measurements [4] show that the height to which ethanol rises is increased by a substantial factor on inserting ethacryl powder of particle diameter 0.03 mm and applying a potential difference of 1000 V, while the rate of rise of the liquid is also substantially increased.

A liquid of high dielectric constant and high zeta potential (alcohol, water, or aqueous solutions of HCl, KCl, or KOH) may be employed [5] to obtain large pressures in electroosmotic pumps; however, some of these are of high conductivity, which prevents the application of strong fields because of heating and electrolysis.

2. Electrohydrodynamic Heat Pipes. These pipes have two different designs: with longitudinal electrodes and with multistage pumping.

In the first case, the effect arises from the liquid being drawn into the space between the electrodes in the condenser, in which a hydrostatic pressure difference is set up [6,7]:

$$\Delta P = \frac{\varepsilon_0(\varepsilon_l - \varepsilon_v)E_e^2}{2} - \frac{\varepsilon_0(\varepsilon_l - \varepsilon_v)E_c^2}{2}. \tag{3}$$

The condition for normal operation of such a device is $E_e > E_c$, which is met by appropriate shaping and disposition of the electrodes. The liquid moves from the condensation zone in response to the electric field in the evaporation zone. The maximum possible pressure difference set up by the electric force (for $E_c = 0$) is

$$\Delta P^{max} = \frac{\varepsilon_0(\varepsilon_l - \varepsilon_v)E^2}{2}, \tag{4}$$

where the field strength is derived from the formula for a planar condenser.

Various designs with longitudinal electrodes have been examined; the electrodes may be strips [7], thin wires [8,9], or rods [10,11], or they may be insulated [12] or bare wires. The electric fields may be steady or alternating because the effects described by (3) and (4) are not dependent on the direction of the field.

Institute of Applied Physics, Academy of Sciences of the Moldavian SSR, Kishinev. Lykov Institute of Heat and Mass Transfer, Academy of Sciences of the Belorussian SSR, Minsk.
Translated from Inzhenerno-Fizicheskii Zhurnal, Vol. 36, No. 6, pp. 1126-1137, June, 1979. Original article submitted April 4, 1978.

 0022-0841/79/3606-0748$07.50 

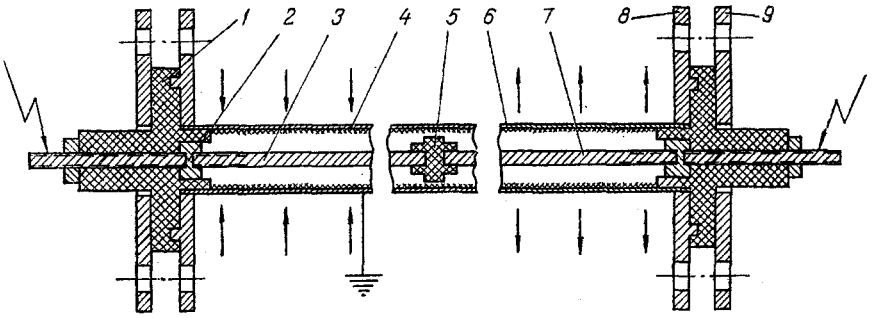


Fig. 1. Electrohydrodynamic heat pipe with longitudinal electrode: 1) supporting insulator; 2) sealing washer; 3, 7) high-voltage electrodes in the evaporation and condensation zones; 4) body; 5) insulating washer; 6) capillary structure; 8, 9) welded and bolted flanges.

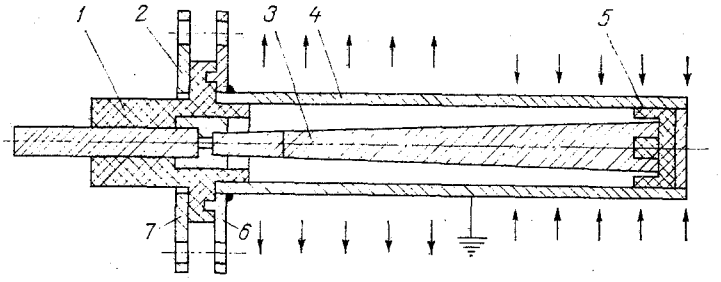


Fig. 2. Electrohydrodynamic heat pipe with varying field strength: 1, 5) insulating washers; 2) sealing washer; 3) high-voltage electrode; 4) body; 6, 7) welded and bolted flanges.

The heat carrier is drawn into the region of strongest field, which ensures that it is supplied to the evaporation zone, but also there may be electroconvection and dispersal in a device with longitudinal electrodes, and these effects can be utilized in controlling the heat transfer, as is clear from researches on condensation and boiling in the presence of electric fields [13-19]. However, there has been no adequate research on the scope for better use of these effects in heat pipes.

We have examined several types of electrohydrodynamic heat pipe, which have yielded very hopeful results. In particular, viability tests have been performed on a very simple design (Fig. 1) [20,21], which may be made of copper (length 1000 mm, diameter 22 mm, and wall thickness 2 mm), with an electric heater of length 100 mm and a condenser of length 150 mm. The wick is provided by E-01 glass cloth of 60% porosity and thickness 3 mm. The design provides for applying electric fields separately to the evaporation and condensation zones. The pipe was tested in a near-horizontal position. The heat carrier was freon 113. An electric field in the evaporation zone produced a substantial fall in the temperature difference along the heat pipe because the carrier was drawn into the space between the electrodes, whereas a field in the condensation zone caused a considerable increase in the temperature difference, sometimes because the field caused the wick to dry out in the evaporation zone.

Such a heat pipe has also been built without a capillary structure (length 120 mm, diameter 19 mm, heater length 50 mm, and condenser length 60 mm), in which the return of the carrier was provided solely by the electric field (Fig. 2). Here again the carrier was freon 113. Inhomogeneity in the electric field was provided by appropriate shaping of the high-voltage electrode, which was a truncated cone whose base lay in the evaporation zone. The body of the heat pipe was grounded. Some results have been published [22] on this heat pipe operating at 45° (against the force of gravity).

The design of another form of pipe has been simplified by providing a field only in the evaporation zone [23], which reduced the temperature difference along the pipe substantially. The measurements were made on a pipe manufactured from copper of length 750 mm and of internal

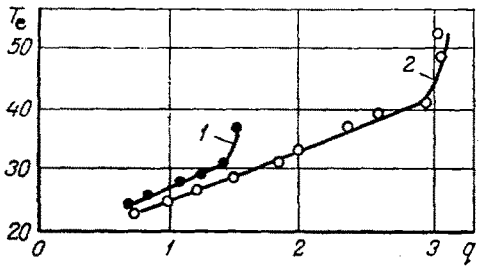


Fig. 3. Mean evaporator temperature $T_e$ (°C) in relation to heat-flux density q ($W/cm^2$): 1) E = 0; 2) 25 kV/cm; Δh = 1 cm.

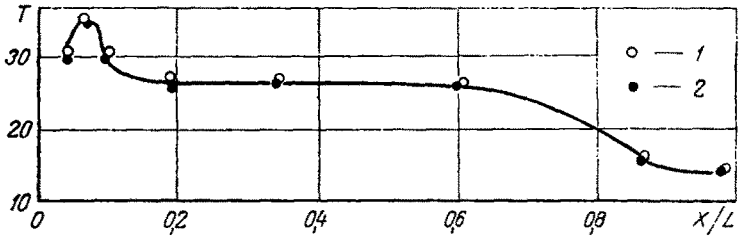


Fig. 4. Distribution of temperature T (°C) along the heat pipe: 1) $E_e$ = 0, Q = 35 W, thermal-syphon mode; 2) $E_e$ = 25 kV/cm, Δh = 1 cm.

diameter 12 mm. The electric heater had a length of 70 mm, while the condenser was a liquid heat-exchanger of length 140 mm. The wick was provided by three layers of 200-μm brass gauze fixed by explosive techniques to the wall of the tube (method developed at this institute). The working medium was freon 113. The high-voltage electrode was a needle of diameter 2 mm and length equal to the length of the evaporation zone. Figure 3 shows the mean temperature of the evaporator as a function of the heat-flux density. The pipe was tested with the evaporator 1 cm above the condenser. A field of 25 kV/cm in the evaporation zone doubled the maximum working heat flux. The transport performance of the wick matched the heat loading for low heat fluxes, and the curves at low fluxes were virtually coincident. Both curves in Fig. 4 correspond to a transferred power of 35 W; in one case the voltage was zero, so the pipe worked as a simple thermal syphon, while in the other case the field was 25 kV/cm, with the evaporator 1 cm above the condenser.

Figure 5 shows the mean temperature difference across the evaporator in relation to the power transferred by the pipe; curve 2 corresponds to thermal-syphon load, while curves 1 and 3 represent the evaporator 1 cm above the condenser for E = 0 and E = 25 kV/cm in the evaporation zone.

These results show that the heat fluxes are those produced in thermal-syphon mode if a heat pipe with longitudinal electrodes is operated with the evaporator slightly above the condenser.

Therefore, the electric field in such a device sets up an additional hydrodynamic pressure difference ΔP as defined by (3) and accelerates the heat transfer in the boiling and condensation zones, while a field applied only to the condensation zone as a rule adversely affects the heat transfer, because liquid is drawn into the condensation zone, with the consequence that the evaporation zone tends to dry out. The transfer characteristics may be readily controlled by means of the field strength. On the other hand, the scope for utilizing field effects is not exhausted in the above designs. From (4) we have that for $\varepsilon_0(\varepsilon_l - \varepsilon_v) = 2\cdot10^{-11}$ F/m, $E^2 = 10^{14}$ V/m² the result is ΔP = $10^3$ N/m² = 10 cm $H_2O$, which is not always adequate for practical purposes.

We can neglect the pressure difference across the vapor phase and write the pressure balance in the following form [24] in evaluating the heat and mass transfer in such a pipe:

$$\Delta P_l + \Delta P_m + \frac{\varepsilon_0(\varepsilon_l - \varepsilon_v)E_c^2}{2} \leqslant \Delta P_{cap} + \frac{\varepsilon_0(\varepsilon_l - \varepsilon_v)E_e^2}{2}. \quad (5)$$

We neglect the inhomogeneity in the capillary structure and rewrite (5) as

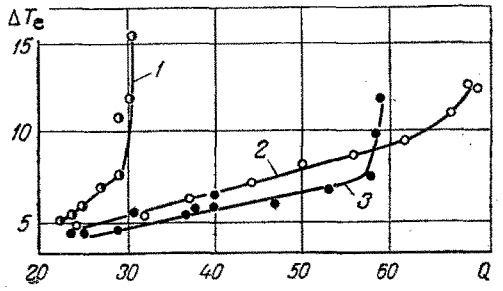


Fig. 5. Mean temperature difference $\Delta T_e$ (°C) at evaporator in relation to power Q (W) transferred by heat pipe: 1) $E_e = 0$, $\Delta h = 1$ cm; 2) $E_e = 0$, $\Delta h < 0$; 3) $E_e = 25$ kV/cm, $\Delta h = 1$ cm.

$$\frac{\eta_l G_l L}{Fk\gamma_l} \pm \gamma_l g L \sin\beta + \frac{\varepsilon_0(\varepsilon_l - \varepsilon_v) E_c^2}{2} \leqslant \frac{4\sigma\cos\theta}{d} + \frac{\varepsilon_0(\varepsilon_l - \varepsilon_v) E_e^2}{2}; \tag{6}$$

$$Q_{max} = \frac{Fkr\gamma_l}{\eta_l L}\left(\frac{4\sigma\cos\theta}{d} + \frac{\varepsilon_0(\varepsilon_l - \varepsilon_v) E_e^2}{2} - \frac{\varepsilon_0(\varepsilon_l - \varepsilon_v) E_c^2}{2} \pm \gamma_l g L \sin\beta\right). \tag{7}$$

Here the minus sign in front of the third term corresponds to the electrohydrostatic head and the head set up by the capillary forces, which may in part balance out, while the minus sign in front of the fourth term corresponds to the case where the gravitational forces prevent the return of the carrier to the evaporation zone.

The following is the electric field in the condensation zone that inhibits the device in the horizontal position for the case $E_e = 0$:

$$E_c = \sqrt{\frac{8\sigma\cos\theta}{d\varepsilon_0(\varepsilon_l - \varepsilon_v)}}. \tag{8}$$

Experiment shows that an electric field applied to the condensation zone with the tube in the horizontal position or with the evaporator slightly above the condenser can be used to switch the pipe on and off.

Equations of Electroconvective Heat Transfer. More efficient heat pipes, including those operating against gravitational forces, can be designed by combining electrohydrodynamic transfer with electroconvective heat transfer. A multistage pump (where the hydrostatic pressure difference is proportional to the number of stages, so the pressure can be adjusted by choice of an appropriate number) also provides for variation of the carrier, the field strength, and the field configuration; this can result in considerable improvement in the performance by comparison with ordinary heat pipes.

Mathematical description of the electrohydrodynamic phenomena and electroconvective heat transfer in such a heat pipe can be based on the following general system of equations [25, 26]:

$$\gamma(\bar{v}\nabla)\bar{v} = -\nabla P + \bar{f} + \gamma\bar{g} + \eta\nabla^2\bar{v}, \tag{9}$$

$$\bar{v}\nabla T = a\nabla^2 T + \sigma_e E^2/c\gamma, \tag{10}$$

$$\nabla\bar{v} = 0, \tag{11}$$

$$\rho = \nabla(\varepsilon_0\varepsilon\bar{E}), \tag{12}$$

$$\bar{E} = -\nabla U, \tag{13}$$

$$\nabla\bar{j} = 0, \tag{14}$$

$$\bar{j} = \sigma_e\bar{E} + \rho\bar{v} - D\nabla\rho, \tag{15}$$

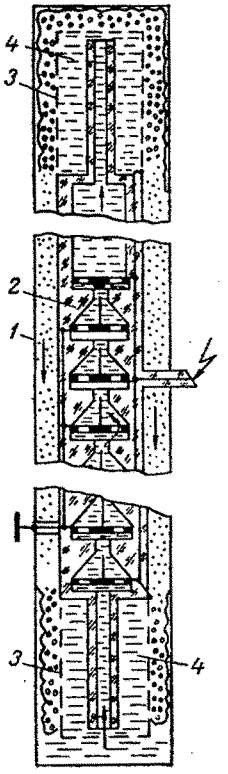


Fig. 6. Electrohydrodynamic heat pipe with multistage electrohydrodynamic pump.

$$\bar{f} = \rho\bar{E} - \frac{\varepsilon_0}{2}E^2\nabla\varepsilon + \frac{\varepsilon_0}{2}\nabla\left[E^2\gamma\left(\frac{\partial\varepsilon}{\partial\gamma}\right)_T\right], \tag{16}$$

$$\sigma_e = \sigma_e(T,\ E), \tag{17}$$

$$\varepsilon = \varepsilon(T,\ E). \tag{18}$$

It follows from (12) and (15) that the following is the Coulomb force for v = D = 0:

$$\bar{f} = \rho\bar{E} = \sigma_e\bar{E}\nabla\tau\bar{E} \tag{19}$$

which arises because the medium is inhomogeneous. The latter in turn may be due to temperature differences or inhomogeneity in the electric field, as is evident from (17) and (18), or else it may be due to heterogeneity in the medium and so on. Here we consider only the electrohydrodynamic phenomena that have been observed in electrohydrodynamic heat pipes.

Needle-Plane Electrohydrodynamic Pump. In this type of pump, electroconvection arises from inhomogeneity in the electric field, and the design is extremely simple (Fig. 6). As the field is inhomogeneous ($\nabla E^2 \neq 0$ on account of the electrode geometry), we have from (12) and (17) that the force is $f \sim \rho E \sim \sigma_e E\nabla\sigma_e(E) \sim \nabla E^2 \neq 0$, and it is readily seen that this is always directed towards the point. If such an electrode system is surrounded by a channel, we get a needle-plane EHD pump.

The operation of such a pump has been discussed [26], and the following equations have been derived for the pressure difference set up in one stage:

$$\Delta P = \frac{j}{b}L + \frac{\varepsilon_0\varepsilon v}{b}\left(\frac{v}{b} + E_{cor}\right) - \frac{\varepsilon_0\varepsilon v}{b}\left[\frac{2j}{\varepsilon_0\varepsilon b}L + \left(\frac{v}{b} + E_{cor}\right)^2\right]^{-\frac{1}{2}} - \xi\frac{\gamma v^2}{2}, \tag{20}$$

where

$$\eta_{opt} = \frac{2}{3}\frac{1}{\sqrt{\frac{3}{2}}\sqrt{\frac{\xi\gamma b^2}{\varepsilon_0\varepsilon}} + 1} \tag{21}$$

is the optimum efficiency; L, distance between the electrodes; $\xi$, loss coefficient; and $E_{cor}$, field at which a corona discharge arises.

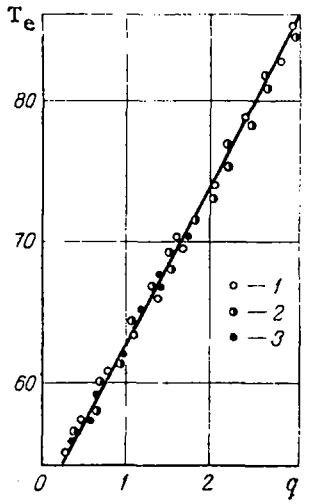


Fig. 7. Mean evaporator temperature as a function of heat-flux density q ($W/cm^2$): 1) thermal-syphon mode; 2) $\Delta h$ = 10 cm, 3) 50.

Equation (20) is inconvenient for engineering calculations, because the current density appears in the argument, and this is dependent on the working conditions, so we consider a simplified form in order to obtain a more convenient formula. The space-charge density in the one-dimensional case is

$$\rho = \varepsilon_0 \varepsilon \frac{dE}{dx}, \tag{22}$$

so

$$E = \frac{\rho}{\varepsilon_0 \varepsilon} x + C. \tag{23}$$

We assume that the electrical relaxation time of the medium is small by comparison with the characteristic time spent by the liquid in the space between the electrodes, i.e., we assume that the liquid flow is completely saturated with charge, so the field strength near the corona electrode is affected by the charge density $\rho$ and may be taken as zero, whereupon C = 0 and

$$E = \frac{\rho}{\varepsilon^0 \varepsilon} x. \tag{24}$$

We assume that $\rho$ = const and put

$$U = \int_0^L E dx = \int_0^L \frac{\rho}{\varepsilon_0 \varepsilon} x dx = \rho L^2 / 2\varepsilon_0 \varepsilon, \tag{25}$$

so

$$\rho = 2\varepsilon_0 \varepsilon U / L^2. \tag{26}$$

The Coulomb force $\rho E$ set up by one stage results in the following pressure difference defined by (24) and (26):

$$\Delta P = \int_0^L \rho E dx = \int_0^L \frac{4\varepsilon_0 \varepsilon U^2}{L^4} x dx = 2\varepsilon_0 \varepsilon U^2 / L^2. \tag{27}$$

We estimate the freon 113 pumping rate in such a pump by means of the Hagen–Pouseille equation for a cylindrical channel on the basis of (27):

$$2\varepsilon_0 \varepsilon U^2 / L^2 = 32 \eta v_{av} L / R^2, \tag{28}$$

so

$$v_{av} = \varepsilon_0 \varepsilon U^2 R^2 / 16 \eta L^3, \tag{29}$$

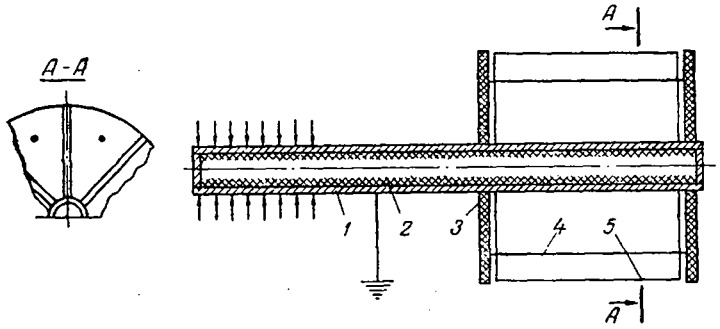


Fig. 8. Heat pipe with electroconvective cooling: 1) body; 2) capillary structure; 3) insulating washers; 4) high-voltage electrodes; 5) cooling fins.

which can provide a pump of handling capacity $2.2 \cdot 10^3$ W with R = 1 mm, U = 20 kV, L = 5 mm, $\varepsilon_0\varepsilon = 2 \cdot 10^{-11}$ F/m, $r = 1.45 \cdot 10^5$ J/kg, and $\eta = 5 \cdot 10^{-4}$ N·sec/m$^2$.

Heat Transfer in Condensation and Boiling in an Electric Field. We consider heat transfer during condensation and boiling [19] in a film in an electric field. This involves examining the hydrodynamics of a liquid partially filling the space between the electrodes and the condenser, which is connected to a high-voltage source, and this has a bearing on an electrohydrodynamic heat pipe because of the partial filling with liquid and the presence of an electric field. There is an interface between phases differing in electrophysical parameters (liquid and vapor), and the external electric field induces charges and produces forces that disperse the liquid, so thin films are produced on the electrodes. The heat transfer can then be determined approximately from

$$\alpha = \lambda/\delta, \tag{30}$$

where $\delta$ is the effective film thickness.

The method of dimensions gives the thickness $\delta$ in an electric field (apart from a constant); it is assumed that $\delta = f(\sigma, \varepsilon_0\varepsilon E^2/2)$, and the above quantities can give only one dimensionless complex $\varepsilon_0\varepsilon E^2\delta/\sigma$, which is assumed to be a function of $\sigma$ and $\varepsilon_0\varepsilon E^2/2$, but it is impossible to form a dimensionless complex from these. Therefore $\varepsilon_0\varepsilon E^2\delta/\sigma$ = const, and so $\delta$ = const $\sigma/\varepsilon_0\varepsilon E^2$, while experiment [19,27] gives

$$\delta = 0.2\,\sigma/\varepsilon_0\varepsilon E^2 = 0.2\sigma/E\rho_s, \tag{31}$$

where $\rho_s$ is the surface charge density.

The boiling and condensation are repetitive, so the surface charge density is dependent on the relation between the characteristic time t and $\tau$ for film renewal, and it is defined by

$$\rho_s = \varepsilon_0\varepsilon_v E\,[1 - \exp(-t/\tau)]. \tag{32}$$

For given heat flux q and thickness $\delta$

$$t = \delta\gamma r/q. \tag{33}$$

If $t/\tau \leq 1$, it is sufficiently accurate to replace $1 - \exp(-t/\tau)$ by $t/(\tau + t)$, and then we take the first two terms in the expansion of $\exp(-t/\tau)$ to get the joint solution of (30), (31) and (33) as

$$\alpha = \frac{2\lambda\varepsilon_0\varepsilon_v E^2\gamma r\tau^{-1}}{0.2\,\sigma\gamma r\tau^{-1} + \sqrt{(0.2\,\sigma\gamma r\tau^{-1})^2 + 0.8\,\varepsilon_0\varepsilon_v E^2\gamma r\tau^{-1}\sigma q}}. \tag{34}$$

This formula is in agreement with experiment [19].

Parameter Measurement. Figure 6 shows a general view of a multistage system in section; the heat pipe consists of the body 1, which encloses the multistage electrohydrodynamic pump 2, with the metallic grids 3 filled with the porous material 4. The arrows indicate the directions of motion of the vapor and liquid.

When the system is connected to a high-voltage supply as shown in Fig. 6, the liquid is pumped into the evaporation region; the porous material 4 causes the material to wet the metal

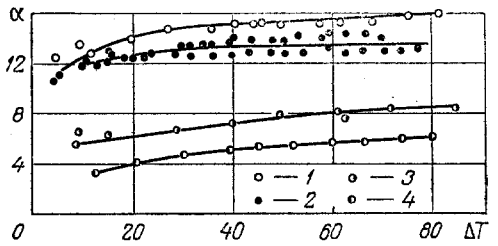


Fig. 9. Heat-transfer coefficient α (W/$m^2$·deg) as a function of wall-air temperature difference ΔT (°C): 1,2) U = 10 kV, horizontal and vertical fins; 3,4) U = 0, horizontal and vertical fins.

grids 3, and the electric field between the body 1 and the grids 3 causes the liquid to disperse over the surface of the evaporator, while the film of condensate in the condenser is withdrawn.

The above theoretical arguments can be applied in calculating the heat-transfer characteristics of such a pipe; the observations were made on a pipe in which the carrier was supplied to the evaporator by an electrohydrodynamic pump and was distributed there by a capillary-channel structure (Fig. 7). The heat-transfer characteristics were almost independent of the orientation. The overall length was 1000 mm, while the evaporation area was 45 $cm^2$, and this served to reproduce the results obtained in thermal-syphon mode with the evaporator at heights up to 50 cm above the condenser.

Electroconvection in External Heat-Pipe Cooling. Most of the studies considered above are concerned with improving the internal characteristics of heat pipes, but it is also necessary to improve the external characteristics in many cooling applications, particularly for electronic and thermoelectric devices. One of the best techniques in this area is to use finned surfaces. Although fins have been widely employed, their performance is often far from perfect in accelerating heat transfer, particularly as concerns the energy consumed in providing the required thermal performance.

However, ribbed tubes usually result in much larger cooling devices, and the desire to minimize dimensions lead us to examine various means of adjusting the hydrodynamic characteristics of heat-carrier flows. Forced air cooling of fins consumes a considerable amount of energy and also reduces the reliability (on account of the pumps and blowers), and therefore we have examined a static device in which free convection at the fins is accelerated by an electric field (electric wind), which is most effective if the field is highly inhomogeneous. The heat pipe of Fig. 8 has a condensation zone in the form of a cylinder of diameter 12 mm and wall thickness 1 mm, which has eight fins of height 40 mm and length 150 mm cooled by free convection in air. The evaporator and the adiabatic zone are thermally insulated. High-voltage electrodes are placed symmetrically between the cooling fins. This pipe was tested in various orientations ranging from horizontal to vertical, where it was assumed that the internal thermal resistance was small by comparison with the external thermal resistance in the condensation zone. The temperature of the heat-transfer surface was measured with copper–constantan thermocouples at the base and crest of a fin. These thermocouples were placed in such a way as to minimize any additional inhomogeneity in the electric field.

Measurements were made (Fig. 9) at 50 Hz and 10 kV; the heat-transfer coefficient was only slightly dependent on the temperature difference, and ΔT less than 10° resulted in Joule heating by the corona current having a considerable effect, so the absolute values of α in this range are somewhat underestimated. The heating of the air by the corona current can be neglected at higher degrees of thermal loading. See [28] for the main results on fin cooling by electric wind methods.

These results show that electrohydrodynamic methods of controlling heat-transfer characteristics of heat pipes are reasonably effective and should find general use.

## NOTATION

L, pipe length; R, radius of channel; $l$ and d, capillary length and diameter; Δh, height of evaporator above condenser; γ, density; r, heat of phase transition; ΔP, pressure drop;

$\eta$, dynamic viscosity; G, flow rate; F, cross section for liquid transport; $\sigma$, surface tension; $\theta$, wetting angle; $\beta$, angle of inclination; Q, heat flux; T, temperature; $a$, thermal diffusivity; c, specific heat; $\alpha$, heat-transfer coefficient; k, permeability; $\lambda$, thermal conductivity; q, heat flux; $\varepsilon_0\varepsilon$, dielectric constant; $\xi$, electrical potential of interface; U, potential difference; E, electric field; $\sigma_e$, specific electrical conductivity; f, power density; g, acceleration due to gravity; $\rho$, space-charge density; j, current density; D, diffusion coefficient; $\tau$, electrical relaxation time; b, carrier mobility. Subscripts: $l$, liquid; v, vapor; e, evaporator; c, condenser; m, mass forces; cap, capillary forces.

## LITERATURE CITED


1. L. L. Vasil'ev and S. V. Konev, "Controlled heat pipes," Inzh.-Fiz. Zh., 32, No. 5 (1977).
2. S. S. Voyutskii, Textbook of Colloid Chemistry [in Russian], Khimiya, Moscow (1975).
3. V. P. Isachenko, V. A. Osipov, and A. S. Sukomel, Heat Transfer [in Russian], Énergiya, Moscow (1969).
4. S. V. Konev, "A study of electrohydrodynamic effects in capillary impregnation," in: Heat and Mass Transfer at Low Temperatures [in Russian], Nauka i Tekhnika, Minsk (1970).
5. Abu-Romia, Possible Application of Electroosmotic Flow Pumping in Heat Pipes, AIAA Paper No. 423 (1971).
6. T. B. Jones, The Feasibility of Electrohydrodynamic Heat Pipes, NASA CR-114392, Colorado State University, Collins, Colorado (1971).
7. T. B. Jones, "Electrohydrodynamic heat pipes," Heat Mass Transfer, May (1973).
8. T. B. Jones and M. P. Perry, "Electrohydrodynamic heat pipes experiments," J. Appl. Phys., 45, No. 5 (1974).
9. T. B. Jones, NASA CR-114498, Experiments with Electrohydrodynamic Heat Pipes, Colorado State University (1972).
10. R. I. Loerke and R. I. Debs, Measurements of the Performance of Electrohydrodynamic Heat Pipes, AIAA Paper, 75-659, 10th Thermophysics Conference (1975).
11. R. I. Loerke and D. R. Sebits, Flat Plate Electrohydrodynamic Heat Pipe Experiments, Colorado State University (1976).
12. V. M. Sych, Inventor's Certificate No. 357427, Byull. Izobret., No. 33, 89 (1972).
13. N. F. Baboi, M. K. Bologa, and K. N. Semenov, "The effects of electric fields on heat transfer in liquids and gases," Elektron. Obrab. Mater., No. 6 (1967).
14. T. B. Johnson, "Effects of an electric field on heat transfer during boiling," Raket. Tekh. Kosmonav., 6, No. 8 (1968).
15. Velkoff and Miller, Teploperedacha, Ser. C, No. 2 (1965).
16. Choy, Teploperedacha, Ser. C, No. 1 (1968).
17. V. M. Buznik, G. F. Smirnov, and B. M. Zamkevich, Tr. Nikolaevsk. Korablestroit. Inst. Teploenergetika, No. 26, Nikolaev (1968).
18. A. B. Didkovskii and M. K. Bologa, "Aspects of film condensation in an electric field," Elektron. Obrab. Mater., No. 2 (1973).
19. O. I. Mardarskii, I. A. Kozhukhar', and M. K. Bologa, "Boiling in a film produced by dispersal in an electric field," Elektron. Obrab. Mater., No. 1 (1978).
20. V. D. Shkilev, M. K. Bologa, and D. V. Marin, "Effects of an electric field on the heat-transfer characteristics of a heat pipe," Elektron. Obrab. Mater., No. 2 (1977).
21. V. D. Shkilev, M. K. Bologa, and D. V. Marin, Inventor's Certificate No. 568809, Byull. Izobret. No. 30 (1977).
22. E. A. Kondyrev, V. D. Shkilev, and M. K. Bologa, "Effects of an electric field on the heat-transfer characteristics of a thermal syphon," Elektron. Obrab. Mater., No. 5 (1977).
23. V. D. Shkilev, "Operation of an electrohydrodynamic heat pipe against gravity," Izv. Akad. Nauk Mold. SSSR, No. 1 (1978).
24. L. L. Vasil'ev, S. L. Vaaz, V. G. Kiselev, S. V. Konev, and L. P. Grakovich, Low-Temperature Heat Pipes [in Russian], Nauka i Tekhnika, Minsk (1976).
25. F. P. Grosu and M. K. Bologa, "Conditions giving rise to electrical convection," Elektron. Obrab. Mater., No. 6 (1968).
26. I. B. Rubashov and Yu. S. Bortnikov, Electrogasdynamics [in Russian], Atomizdat, Moscow (1971).
27. P. R. Brasier-Smith, Phys. Fluids, 14, 1, 1-6 (1971).
28. M. K. Bologa, V. D. Shkilev, and E. A. Kondyrev, "Electroconvective cooling of a heat pipe," Elektron. Obrab. Mater., No. 1 (1978).